Robust space–time adaptive processing (STAP) in non-Gaussian clutter environments

P.Tsakalides and C.L.Nikias

Abstract: The problem of space–time adaptive processing (STAP) in non-Gaussian clutter is addressed. First, it is shown that actual ground clutter returns are heavy-tailed, and their statistics can be accurately characterised by means of alpha-stable distributions. Then, a new class of adaptive beamforming techniques is developed, based on fractional lower-order moment theory. The proposed STAP methods adjust the radar array response to a desired signal while discriminating against non-Gaussian heavy-tailed clutter modelled as a stable process. Experimental results with both simulated and actual clutter data show that the new class of STAP algorithms performs better than current gradient descent state-of-the-art methods, in localising a target both in space and Doppler, and thus offers the potential for improved airborne radar performance in STAP applications.

1 Introduction

Future advanced radar systems must be able to detect, identify, and estimate the parameters of a target in severe interference backgrounds. As a result, the problem of clutter and jamming suppression has been the focus of considerable research in the radar engineering community [1–3]. Brennan *et al.* considered airborne moving target indication (MTI) radar systems and proposed an adaptive array structure that compensates for near-field scatterers and is able to null out discrete active interference sources [4]. That work is considered as the precursor of modern space–time adaptive processing (STAP) systems. In the context of airborne and shipboard radar, STAP refers to a class of signal processing algorithms that provide improved target detection and parameter estimation in the presence of natural clutter and interference, through the adaptive nulling of both ground clutter and hostile electronic countermeasures or jamming [4–9].

Typically, STAP means the simultaneous processing of the spatial signals received by multiple elements of an array antenna, and the temporal signals provided by the echoes from multiple pulses of a pulse-Doppler radar coherent processing interval (CPI). Hence, space–slow time adaptive processing can be thought of as a combined beamformer and Doppler filter bank. The STAP filter coefficients are adaptively computed using the radar return data so as to provide good estimates of the interference that is present at any given time. The STAP filter weights are regularly updated to track changes in the interference environment. STAP provides improved cancellation of mainlobe clutter, thereby reducing the velocity blind zone and improving the detection of both low-velocity and fast targets. In addition, space–fast time adaptive processing can provide cancellation of terrain scattered jamming. Therefore, STAP also provides detection of targets obscured by sidelobe clutter, and detection in environments of both 'hot' clutter or multipath jamming. Finally, adaptivity provides robustness to system errors and reduces the sensitivity to miscalibration problems. As a result, STAP technology is considered as pivotal for the development of the next generation of airborne radar surveillance systems.

Adaptive statistically optimum beamformers maximise the signal-to-noise ratio of the array output for optimal signal detection. The multiple sidelobe canceller (MSC) is perhaps the earliest statistically optimum beamformer, introduced by Applebaum *et al.* [10]. Widrow *et al.* studied the adaptive antenna problem by minimising the mean square error between the beamformer output and a reference signal [11]. Reed *et al.* concentrated on adaptive radar applications. They developed an adaptive processor which maximises the probability of detection for a fixed false alarm rate [1]. They also introduced a direct method of adaptive weight computation, based on the sample covariance matrix of the noise field, which provides rapid convergence [2].

Although it is anticipated that novel adaptive space–time processing will offer improved detection and false alarm control over classical techniques, and will be preferred whenever the signal processing design assumptions are valid, a dynamically changing environment makes the judicious selection of reference data essential for both detection and parameter estimation. Indeed, it is recognised that effective clutter suppression can be achieved only on the basis of appropriate statistical modeling. Most of the earlier theoretical work in detection and estimation for radar applications has focused on the case where clutter is assumed to follow the Gaussian model. The Gaussian assumption is frequently motivated by the fact that it often leads to mathematically tractable solutions.

In recent years, the radar community has shown extensive interest in the modelling of non-Gaussian clutter by

IEE Proceedings online no. 19990233
DOI: 10.1049/ip-rsn:19990233

Paper first received 18th March and in revised form 23rd September 1998

The authors are with the Signal & Image Processing Institute, Department of Electrical Engineering - Systems, University of Southern California, Los Angeles, CA, USA 90089-2564, USA

considering Weibull, log-normal, and K-distribution models [12–15]. As a result, new radar detectors have been proposed for non-Gaussian environments [16–19]. However, to date, most existing STAP algorithms have been designed assuming Gaussian statistics. Spikes due to clutter sources such as ocean waves, and glints due to reflections from large flat surfaces such as buildings or vehicles are usually present in radar returns. A statistical model of impulsive interference has been proposed, which is based on the theory of symmetric alpha-stable ($S\alpha S$) random processes [20–22]. The model is of a statistical-physical nature and has been shown to arise under very general assumptions, and to describe a broad class of impulsive interference. In particular, it was shown in [20] that the first order distribution of the amplitude of the radar return follows a $S\alpha S$ law, while the first order joint distribution of the quadrature components of the envelope of the radar return follows an isotropic stable law.

Recently, we developed robust techniques for source detection and localisation in the presence of noise, modelled as a complex isotropic stable process [23]. First, we presented optimal, maximum likelihood-based approaches, and derived Cramér–Rao bounds for the additive Cauchy clutter scenario to assess the best-case estimation accuracy which can be achieved [24]. In addition, we developed subspace methods based on fractional lower-order statistics for radar applications, where reduced computational cost is a crucial design parameter [25].

In this paper, we introduce a new STAP beamformer based on a constrained least mean p-norm (LMP) algorithm. The new LMP beamformer is designed to iteratively adapt the weights of a space-time sensor array, so as to minimise the pth-order moment ($p < 2$) of the array output, while maintaining a specific response in the look direction/Doppler. The algorithm is applicable to radar processing problems where the existing interference is impulsive in nature and can be modeled as an alpha-stable process.

In Section 2, we present some necessary preliminaries on alpha-stable theory. In addition, we present results on the modeling of actual radar clutter data by means of alpha-stable distributions. In Section 3, we formulate the space-time adaptive processing (STAP) problem for airborne radar. In Section 4, we present the second-order and our proposed lower-order moments approach to the adaptive beamforming problem. Finally, in Section 5, the improved performance of the new adaptive beamforming method in the presence of impulsive noise is demonstrated via experiments with simulated and actual clutter data series.

2 Alpha-stable statistical models for advanced STAP systems

For decades, heavy-tailed processes have been studied by statisticians and mathematicians. Many of the theoretical advances for an important family of heavy-tailed distributions, the so-called alpha-stable family, are summarised in the monograph on stable non-Gaussian random processes by Samorodnisky and Taqqu [21]. For engineering applications, alpha-stable statistical models and their corresponding fractional lower-order statistics (FLOS) comprise a newly emerging and rapidly expanding signal processing methodology, as underlined by Nikias and Shao [20].

The class of alpha-stable distributions, a natural generalisation of the Gaussian distribution, has some important characteristics which make it very attractive for modelling a wide range of signal and noise environments. This class of distributions is best defined by its characteristic function:

$$\varphi(\omega) = \exp(j\delta\omega - \gamma|\omega|^{\alpha}) \tag{1}$$

where α is the characteristic exponent restricted to the values $0 < \alpha \leq 2$, δ ($-\infty \delta < \infty$) is the location parameter, and γ ($\gamma > 0$) is the dispersion of the distribution. The dispersion parameter γ determines the spread of the distribution around its location parameter δ, in much the same way the variance of the Gaussian distribution determines the spread around the mean. The characteristic exponent α is the most important parameter of the $S\alpha S$ distribution, and it determines the shape of the distribution (see Fig. 1). The smaller the characteristic exponent α, the heavier the tails of the alpha-stable density. This implies that random variables following alpha-stable distributions with small characteristic exponents are highly impulsive. It is this heavy-tail characteristic that makes the alpha-stable densities appropriate for modelling signals and clutter or interference, which are impulsive in nature. We should also note here that the stable distribution corresponding to $\alpha = 2$ coincides with the Gaussian density. In addition, alpha-stable densities obey two important properties which further justify their role in data modelling:

- The stability property, which states that the weighted sum of independent alpha-stable random variables is again stable with the same characteristic exponent α.
- The generalised central limit theorem (GCLT), which states that stable models are the *only* distributions which can be the limit distributions of independent and identically distributed random variables.

In other words, GCLT implies that if the observed randomness is the result of many cumulative effects (as is the case in ambient noise formation due to reflections from many scatterers), and these effects follow a heavy-tailed distribution, then a stable model may be appropriate. In addition, unlike the Gaussian distribution which is symmetric about its mean, stable distributions may also be asymmetric, i.e., they admit skewness. Therefore, in certain applications where a heavy-tailed and asymmetric model is called for, the stable model is a viable alternative to the Gaussian distribution.

An important difference between the Gaussian and other distributions of the alpha-stable family, is that only moments of order less than α exist for the non-Gaussian

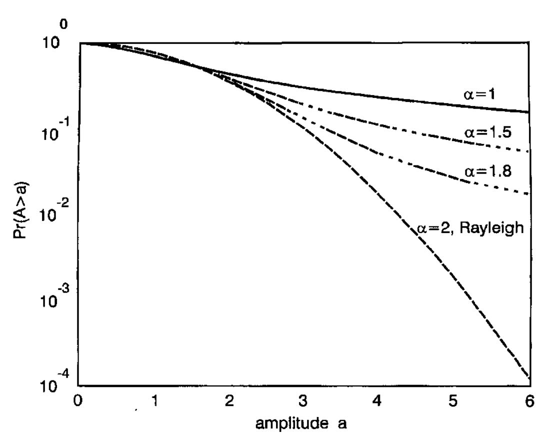

Fig. 1 *Symmetric alpha-stable amplitude probability density functions ($Pr\,(A > a)$)*

Dispersion is $\gamma = 1$ and characteristic exponent is $\alpha = 1.0$, 1.5, 1.8, and $\alpha = 2.0$ (Rayleigh) alpha-stable family members. The *fractional lower order moments* (FLOMs) of an alpha-stable random variable with zero location parameter and dispersion γ are given by:

$$E|X|^p = C(p, \alpha)\gamma^{\frac{p}{\alpha}} \text{ for } 0 < p < \alpha \quad (2)$$

where $C(p, \alpha)$ is a constant depending only on p and α.

In the theory of second-order processes, the concepts of variance and covariance play the important roles of norms in problems of linear prediction, filtering and smoothing. Since non-Gaussian alpha-stable processes do not possess finite pth-order moments for $p \geq \alpha$, covariances do not exist on the space of alpha-stable random variables. For a zero location alpha-stable random variable X with dispersion γ, the *norm* of X is defined as

$$||X||_\alpha = \begin{cases} \gamma^{1/\alpha} & 1 \leq \alpha \leq 2 \\ \gamma & 0 < \alpha < 1 \end{cases} \quad (3)$$

Hence, the norm $\|X\|_\alpha$ is basically a scaled version of the dispersion γ. If X and Y are jointly alpha-stable, the distance between X and Y is defined as

$$d_\alpha(X, Y) = ||X - Y||_\alpha \quad (4)$$

Combining eqns. 2 and 3, it is easy to see that

$$d_\alpha(X, Y) = \begin{cases} (E(|X - Y|^p)/C(p, \alpha))^{1/p} & 0 < p < \alpha, 1 \leq \alpha \leq 2 \\ (E(|X - Y|^p)/C(p, \alpha))^{\alpha/p} & 0 < p < \alpha, 0 < \alpha < 1. \end{cases} \quad (5)$$

Thus, the pth-order moment of the difference between two alpha-stable random variables is a measure of the distance d_α between these two random variables. In the case of $\alpha = 2$ (Gaussian), this distance is half the variance of the difference. In addition, all fractional lower-order moments of an alpha-stable random variable are equivalent, i.e., the pth and qth-order moments differ by a constant factor, independent of the random variable for $p, q < \alpha$. Furthermore, it was shown by Schilder [26] that for $1 \leq \alpha \leq 2$, $\|\cdot\|_\alpha$ defined in eqn. 3 is a norm in the linear space of alpha-stable processes.

From the above discussion, it is clear that in alpha-stable theory, the minimum dispersion (MD) criterion can play a role analogous to the minimum mean-square error (MMSE) criterion in second-order moments theory. In other words, the generic estimation problem of stable processes can be formulated as finding an element $\hat{Y}$ in the linear space $L(X(t), t \in T)$ of the observations $\{X(t), t \in T\}$, such that

$$||Y - \hat{Y}||_\alpha = \min_{Z \in L(X(t), t \in T)} ||Y - Z||_\alpha \quad (6)$$

or equivalently

$$E|Y - \hat{Y}|^p = \min_{Z \in L(X(t), t \in T)} E|Y - Z|^p \text{ for } 0 < p < \alpha \quad (7)$$

For $0 < \alpha < 2$, $L(X(t), t \in T)$ is a Banach space, and $\hat{Y}$ always exists and is unique. Our proposed STAP methodology uses extensively the notion of fractional lower order moments to achieve robust clutter suppression and target detection. The fundamental motivation for doing so is our finding that radar signal processing algorithms based on FLOMs are robust in various ambient noise and interference environments. In a related work, we used the notion of covariation (lower order cross-correlation) to obtain robust joint spatial and Doppler-frequency high-resolution estimates in heavy-tailed clutter [25, 27]. In this paper, we explore the FLOM notion to design an adaptive space–time processor for robust target detection in severe clutter.

Next, we show that the statistical characteristics of radar returns are decidedly non-Gaussian, and instead can be accurately modeled by means of stable distributions. The reason is that the characteristic exponent α allows us to represent signals and/or noise with a continuous range of impulsiveness. Figs. 2–5 show results on the modelling of the amplitude statistics of real radar clutter data by means of the Rayleigh, $S\alpha S$, K, and Weibull distributions. The clutter data were provided by Rome Laboratory and are part of the Moutaintop Database [28]. The clutter data set contains monostatic clutter measured using the Radar Surveillance Technology Experimental Radar (RSTER). The data were collected on 27 August, 1993 as part of the Clutter Map Multi-Frequency Experiment. The waveform employed was a 5 μs pulsed CW signal at 435 MHz. The measurements are unequalised I/Q data, and they cover a range from 3.5 to 115 nmi. Figs. 2 and 3 depict the in-phase and quadrature components of the clutter corresponding to $\theta = 315°$ in azimuth and $[r_{min}\ r_{max}] = [3.5\ 80.0]$ nmi in range. Figs. 4 and 5 present the modelling in terms of both the probability density function (PDF) and the amplitude probability density (APD) $Pr\{X > x\}$. The figures demonstrate that the stable distribution is superior to the Rayleigh, K, and Weibull distributions for modelling the tails of the particular radar clutter data under study.

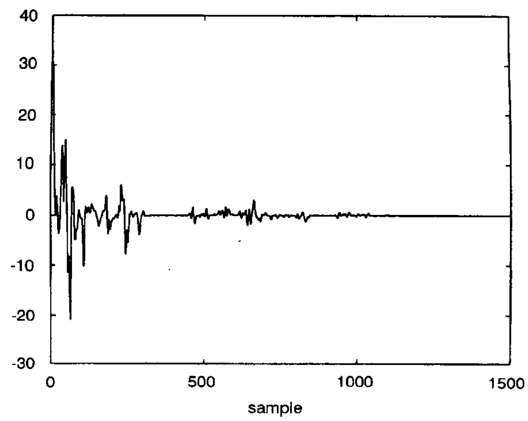

Fig. 2 *Real part of the Mountaintop clutter data corresponding to* $\theta = 315°$ *in azimuth and* $[r_{min}\ r_{max}] = [3.5\ 80.0]$ *nmi in range*

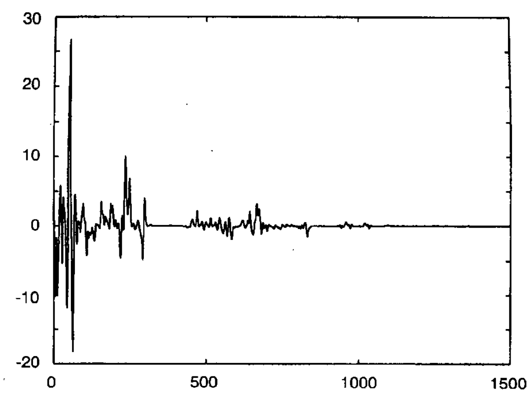

Fig. 3 *Imaginary part of the Mountaintop clutter data corresponding to* $\theta = 315°$ *in azimuth and* $[r_{min}\ r_{max}] = [3.5\ 80.0]$ *nmi in range*

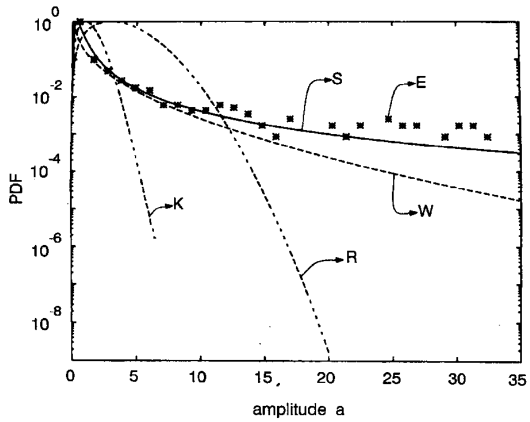

Fig. 4 *Probability density function comparison function*
E = empirical; K = K distribution; R = Rayleigh; S = SαS; W = Weibull

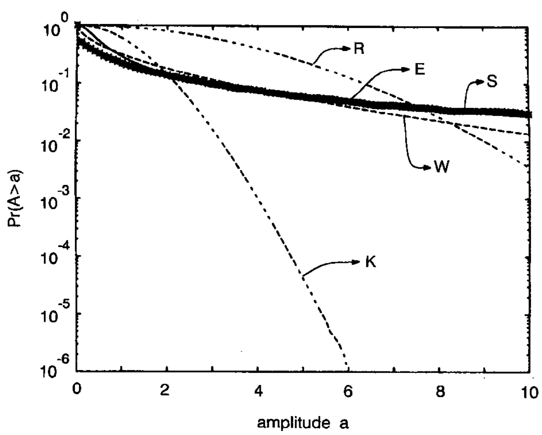

Fig. 5 *Amplitude probability density comparison probability*
E = empirical; K = K distribution; R = Rayleigh; S = SαS; W = Weibull

Compared with existing statistical models for ambient noise and interference, signal processing algorithms based on alpha-stable models for detection, parameter estimation, and array processing demonstrate robustness even in the presence of mismatches in the assumed conditions of noise and interference [20]. In addition, the use of fractional lower-order statistics and covariations is indeed very simple to understand and implement in real-time processing scenarios.

3 STAP problem formulation

Space–time adaptive processing (STAP) has been introduced as a generalisation of displaced-phase-centre antenna (DPCA) processing and has been recognised as the technology which will enable long-range detection of increasingly smaller targets in the presence of severe clutter and jamming. STAP refers to adaptive antenna processors which simultaneously combine the signals received on multiple elements of an antenna array, and from multiple pulse repetition periods of a radar coherent processing interval [4, 29]. In other words, the STAP processor can be viewed as a two-dimensional (2-D) filter, which performs both beamforming (spatial filtering) and Doppler (temporal) filtering to suppress interference and achieve target detection and parameter estimation.

In the following, we present a model for the signal received by an airborne pulsed-Doppler radar. The system under consideration is a pulsed-Doppler radar residing on an airborne or shipboard platform. The radar antenna is a uniformly spaced linear array antenna consisting of N elements, spaced d metres apart, that transmit a coherent burst of M pulses at a constant pulse repetition frequency (PRF) $f_r = 1/T_r$, where T_r is the pulse repetition interval (PRI).

Radar returns are collected over a coherent processing interval (CPI) of length MT_r. For each PRI, L time (range) samples are collected to cover the range interval. This multidimensional data set is visualized as the $N \times M \times L$ cube of complex samples shown in Fig. 6. Then, the data at a certain range of interest l corresponds to a slice of the CPI datacube. This slice is an $N \times M$ space–time snapshot, denoted by $\mathbf{X}$, which consists of the spatial snapshots for all pulses in the range of interest:

$$\mathbf{X}_l = [\mathbf{x}_{0,l}, \mathbf{x}_{1,l}, \ldots, \mathbf{x}_{M-1,l}] \tag{8}$$

where $x_{m,l}$ is the $N \times 1$ vector of antenna element outputs, or a spatial snapshot, at the time of the lth range gate and mth pulse [29]. Hence, the rows of $\mathbf{X}_l$ represent the temporal (pulse-by-pulse) samples for each antenna element. It is convenient to write the data for a single range gate as the lth $MN \times 1$ vector χ_l, termed the '*space–time snapshot*,' by stacking the columns of $\mathbf{X}_1$.

Each return χ (we drop the range index l for notational convenience) encompasses components due to the target, the interference sources or jammers, the clutter, and the white noise, respectively:

$$\chi = \chi_t + \chi_j + \chi_c + \chi_w \tag{9}$$

Assuming the existence of a point target at angle ϕ_t with Doppler frequency f_t the corresponding component of the space–time snapshot is given by [29]:

$$\chi_t = \alpha_t \mathbf{v}(\psi_t, \omega_t) \tag{10}$$

where α_t is the amplitude of the target, $\psi_t = 2\pi(d/\lambda_0)\sin(\phi_t)$ is the normalised angle, $\omega_t = 2\pi(f_t/f_r)$ is the normalised Doppler, and $\mathbf{v}(\psi_t, \omega_t) = \mathbf{b}(\omega_t) \otimes \mathbf{a}(\psi_t)$ is the $MN \times 1$ *space–time steering vector* that can be expressed as the Kronecker matrix product of $\mathbf{b}(\omega_t) = [1, e^{-j\omega_t}, \ldots, e^{j(M-1)\omega_t}]^T$, the $M \times 1$ *temporal steering vector,* and $a(\psi_t) = [1, e^{-j\psi t}, \ldots, e^{-j(N-1)\psi_t}]^T$, the $N \times 1$ *spatial steering vector.*

The jamming environment consists of several sources that are assumed to be temporally white (barrage jammers spread over all Doppler frequencies at a particular

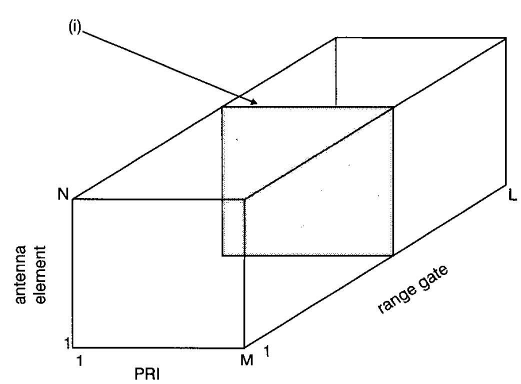

Fig. 6 *Three-dimensional CPI Datacube*
(i) N × M dimensional range gate of interest

azimuth). Hence, jamming looks like thermal noise in the time domain, but like a discrete clutter source in the spatial domain. Then, the space–time snapshot component due to a jammer located at angle ϕ_j is given by

$$\chi_j = \alpha_j \otimes \mathbf{a}(\psi_j) \tag{11}$$

where $\alpha_j = [\alpha_0, \alpha_1, \ldots, \alpha_{M-1}]^T$ is the $M \times 1$ random vector containing the jammer amplitudes.

Radar clutter is defined as the echoes from any scatterers, not considered to be of tactical significance. When considering a target at a given range, the clutter returns will come from all areas at a so-called ambiguous range R_i, corresponding to the range gate of interest. As an approximation to a continuous field of clutter, the clutter returns for each ambiguous range will be modelled as a superposition of a large number N_c of independent clutter sources, that are evenly distributed in a circular ring about the radar platform. The location of the *ik*th clutter patch is described by its azimuth ϕ_k and ambiguous range R_i. Assuming that the normalised Doppler frequency of the *ik*th patch is ω_{ik}, the clutter component of the space-time snapshot is given by

$$\chi_c = \sum_{i=1}^{N_r} \sum_{k=1}^{N_c} \alpha_{ik} \mathbf{v}(\psi_{ik}, \omega_i k) \tag{12}$$

where α_{ik} is the random amplitude from the *ik*th clutter patch, and N_r denotes the number of range ambiguities. Finally, the component χ_ω in the space–time snapshot is due to the thermal noise present at the sensor elements, and it is spatially and temporally white.

4 STAP based on lower order statistics

The problem of tracking a weak moving target in the presence of strong interferences using radar arrays is known to be one of the most important in radar processing. In the following, we first describe an array weight adaptation algorithm, which minimises the power at the array output while maintaining a chosen frequency response in the angle–Doppler values of interest [30]. Then, we propose an adaptation process based on the minimisation of the dispersion of the array output, for applications where impulsive clutter and jamming signals can be modelled as stable processes. The use of the minimum dispersion criterion is justified, as it has been shown that minimising the dispersion is equivalent to minimising the average magnitude and the probability of large estimation errors [31].

4.1 Minimum variance distortionless response (MVDR) STAP

The basic idea behind MVDR STAP is to constrain the response of the processor so that signals with the direction and Doppler of interest are passed undistorted. In fully adaptive STAP, the *MN* array weights $\mathbf{w}$ are chosen to minimise the output variance subject to appropriate linear constraints. The problem is formulated as follows:

$$\min E\{|y|^2\} \text{ such that } \mathbf{C}^H \mathbf{w} = \mathbf{f} \tag{13}$$

where $\mathbf{C}$ is the constraint matrix, which encompasses all the steering vectors with angles and Doppler corresponding to targets of interest and to jammers that we want to suppress. The vector $\mathbf{f}$ has the desired constraining values, and $y(t)$ is the space-time filter output:

$$y(t) = \mathbf{w}^H \chi(t) \tag{14}$$

By using Lagrange multipliers, the optimum space-time filter is shown to be [30]:

$$\mathbf{w}_{\text{opt}} = \mathbf{R}_x^{-1} \mathbf{C} [\mathbf{C}^H \mathbf{R}_x^{-1} \mathbf{C}]^{-1} \mathbf{f} \tag{15}$$

Direct application of eqn. 15 implies knowledge of the correlation matrix $\mathbf{R}_x$ of the array output vector. In most practical situations, the operating environment is non-stationary, and an estimate of the weight vector $\mathbf{w}$ must be recomputed periodically. An adaptation procedure for the beamformer weights was proposed by Frost [30], based on a gradient-descent constrained least mean-squares (LMS) algorithm, and it requires that only the direction and Doppler values of interest be specified *a priori:*

$$\begin{gathered} \mathbf{w}(0) = \mathbf{F} \\ \mathbf{w}(t+1) = \mathbf{P}[\mathbf{w}(t) - \mu y^*(t)\chi(t)] + \mathbf{F} \end{gathered} \tag{16}$$

with

$$\begin{gathered} \mathbf{P} = \mathbf{I} - \mathbf{C}[\mathbf{C}^H \mathbf{C}]^{-1} \mathbf{C}^H \\ \mathbf{F} = \mathbf{C}[\mathbf{C}^H \mathbf{C}]^{-1} \mathbf{f} \end{gathered}$$

where $\mathbf{P}$ is a projection operator to the constraint subspace, $\mathbf{F}$ lies in the constraint hyper-plane (the space spanned by the columns of the constraint matrix $\mathbf{C}$), and μ is a small positive step-size parameter which controls the rate of change of the weight vector $\mathbf{w}(t)$. The constrained LMS algorithm has a self-correcting feature, and adaptively learns the statistics of the clutter. Discussion of the geometric interpretation of the algorithm and its convergence performance to the optimum weight vector can be found in [30].

4.2 Lower order statistics formulation: the LMP STAP algorithm

Since $S\alpha S$ processes do not possess finite *p*th-order moments for $p > \alpha$, traditional beamforming techniques employing second and higher order moments cannot be applied in impulsive noise environments modelled under the stable law. Instead, properties of fractional lower order moments should be used. Hence, for radar systems operating in severe clutter environments, we propose the minimisation of the dispersion of the array output subject to a set of linear constraints.

According to eqn. (2), minimising the dispersion is equivalent to minimising the *p*th-order moment of the array output:

$$\min E\{|y|^p\} \text{ such that } \mathbf{C}^H \mathbf{w} = \mathbf{f} \tag{17}$$

for any $p < \alpha$, with α being the parameter of the associated stable distribution that best describes the clutter statistics. Unlike the optimisation problem described in the previous section, there is no closed form solution to the problem shown in eqn. 17. Therefore, an iterative scheme based on a stochastic gradient method can be used to adapt the array weights [32]. The adaptation procedure for the STAP weights can be derived to be as follows:

$$\begin{gathered} \mathbf{w}(0) = \mathbf{F} \\ \mathbf{w}(t+1) = \mathbf{P}[\mathbf{w}(t) - \mu |y(t)|^{p-2} y^*(t)\chi(t)] + \mathbf{F} \end{gathered} \tag{18}$$

where

$$\begin{gathered} \mathbf{P} = \mathbf{I} - \mathbf{C}[\mathbf{C}^H \mathbf{C}]^{-1} \mathbf{C}^H \\ \mathbf{F} = \mathbf{C}[\mathbf{C}^H \mathbf{C}]^{-1} \mathbf{f} \end{gathered}$$

We will refer to the beamformer described in eqn. 18 as the least mean *p*-norm STAP (LMP STAP) beamformer. Observing eqn. 18 more closely, we see that it is a stochastic gradient descent method with a variable step-size $\mu(t)$, where

$$\mu(t) = \mu_0 \frac{1}{|y(t)|^{2-p}}$$

and $p < \alpha$. A conservative choice for μ_0 in the range of 10^{-2} and 10^{-3} ensures the convergence of the algorithm.

Although, in theory, all pth-order moments are equivalent for stationary environments described by a specific α, as long as $0 < p < \alpha$, in practice, when applying the LMP STAP method, p should be chosen as slightly less (i.e., 0.1–0.3) than the estimated value of α. By changing the parameter p, we obtain a class of LMP STAP algorithms. As a result, this class of STAP methods provides considerable flexibility, which can be useful for optimisation purposes in the presence of non-stationary clutter and jamming environments. Note that when $p = 2$, we obtain the LMS STAP beamformer, while when $p = 1$, the above algorithm coincides with the well-known signed LMS algorithm. The L_p norm has been used in the past within several contexts, such as deconvolution problems in seismic applications [33, 34], and spectral estimation [35]. In radar applications, it can offer better localisation results in certain impulsive noise types.

In concluding this Section, we should point out that a great amount of research has been done regarding the implementation of optimum in the mean-square error (MSE) sense processors in actual radar array applications. Classic Wiener filtering theory, based on second order statistics of the array output, results in optimum STAP weights that are given in a closed form, involving the inverse of the data correlation matrix (see eqn. 15). In non-stationary environments, the inverse of the correlation matrix has to be estimated from small data sizes. Reed *et al.* suggested that a sample matrix inversion (SMI) technique (block adaptation) is more efficient in terms of convergence and data required than stochastic gradient descent algorithms (sample-by-sample adaptation) such as the LMS [2]. On the other hand, the use of non-MSE optimisation criteria see eqn. 17) in filter design usually results in optimal weights that cannot be expressed in closed-form. In this case, tracking the optimal solution in a non-stationary environment can only be achieved with a gradient descent approach.

5 Experimental results

For the purpose of our analysis, the presumed target is located at 20° azimuth with normalised Doppler frequency 0.25. This target has a signal-to-noise ratio (SNR) of 0 dB, representing a small constant radar cross-section target. The interference environment consists of two jammers, clutter and thermal noise. The two barrage jammers are present at $-20°$ and 45° azimuth. The jammer-to-noise ratio (JNR) is set at 30 dB. The clutter-to-noise ratio (CNR) is also set at 30 dB.

The radar adaptive processors consist of 10 elements and 7 pulses in a coherent processing interval (CPI). Hence, the corresponding weight vector is of dimension 70×1. In the following, we compare the performance of the two STAP processors, namely the MVDR STAP (Frost gradient descent) and our proposed LMP STAP, in the presence of interference with varying statistical characteristics. The interference (jammer plus clutter) statistics are described by the alpha-stable family of distributions, that is parameterised by the characteristic exponent α, which takes values between 0 and 2. When $\alpha = 2$, the environment is Gaussian. The smaller the value of α, the more impulsive the nature of the interference.

Both the MVDR and the LMP STAP (with $p = 1.2$) processors are constrained to have unit response at the direction and Doppler of the presumed target. In other words, the constraint matrix C is in fact the space–time steering vector v(20°, 0.25), and the constraints in eqn. 13 and 17 take the form:

$$\mathbf{v}^H(20°, 0.25)\mathbf{w} = 1 \qquad (19)$$

Given the weight vectors produced by the MVDR STAP and the LMP STAP, their response as a function of angle and Doppler is one indicator of the processor performance. This response is called the adapted pattern, and is defined by

$$P_{\mathbf{w}}(\psi, \omega) = |\mathbf{w}^H \mathbf{v}(\psi, \omega)|^2 \qquad (20)$$

where w is the adapted weight vector, and $\mathbf{v}(\psi, \omega)$ is the space–time vector steered at azimuth ψ and Doppler ω. The adapted pattern is a two-dimensional angle–Doppler frequency response. Ideally, the adapted pattern should have nulls in the directions of the interference sources and high gain at the angle and Doppler of the presumed target.

Our results clearly demonstrate that the LMP STAP exhibits detection and estimation performance that is more robust than the performance of MVDR STAP, in a

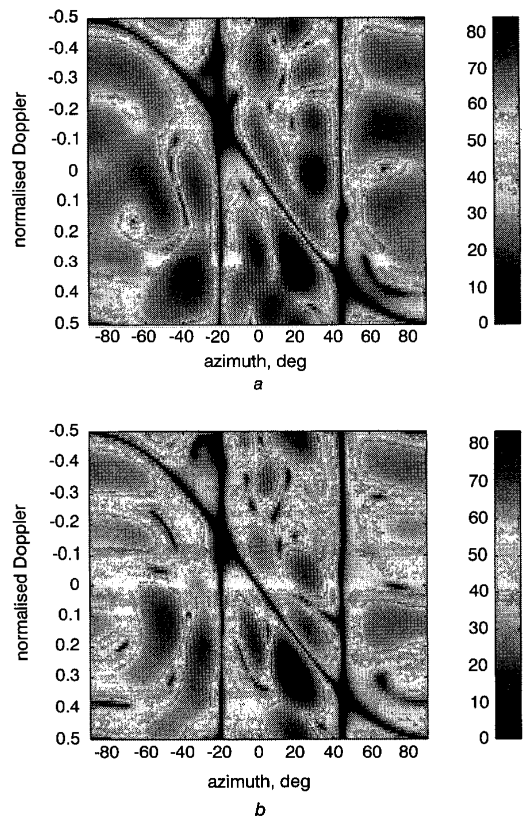

Fig. 7 *Adapted patterns (two-dimensional angle–Doppler frequency responses) for MVDR STAP and LMP STAP*

The presumed target is located at 20° azimuth with normalized Doppler frequency 0.25. The statistics of the clutter (CNR = 30dB) and noise (SNR = 0dB) follow the Gaussian distribution ($\alpha = 2$). Both methods place strong nulls along the two jammers present at $-20°$ and 45° azimuth and along the clutter ridge.
a MVDR STAP
b LMP STAP

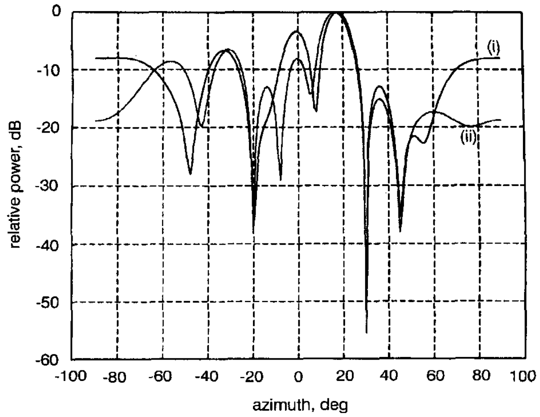

Fig. 8 *Principal cuts at target Doppler*
Note the nulls at both jammer azimuths (− 20° and 45°) and at 30° where the sidelobe clutter has the same Doppler as the target
(i) MVDR STAP; (ii) LMP STAP

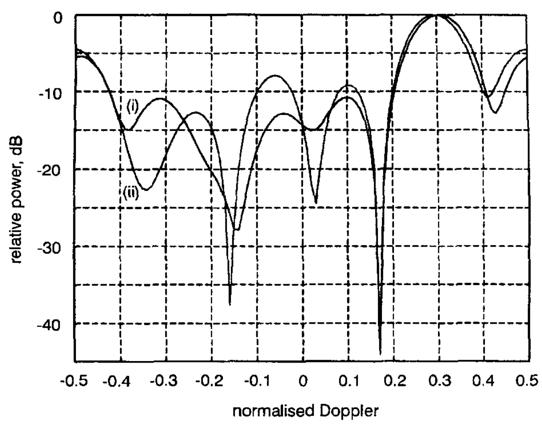

Fig. 9 *Principal cuts at target azimuth*
The null present at approximately 0.18 Doppler suppresses mainlobe clutter
(i) MVDR STAP; (ii) LMP STAP

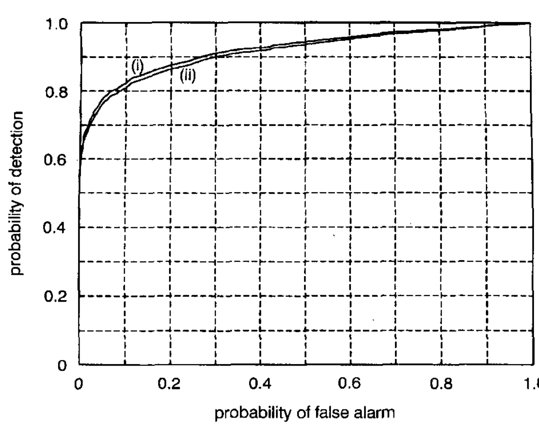

Fig. 10 *Receiver operating characteristics (ROCs) corresponding to the adapted patterns shown in Fig. 7*
(i) MVDR STAP; (ii) LMP STAP

wide range of interference environments. Fig. 7 shows the adapted patterns for the case of Gaussian interference ($\alpha = 2$). The mainlobes of both patterns are at the target location. The jamming signals are suppressed by the deep vertical pattern nulls at the jammer azimuths. In addition, the patterns have a slanted null that spans the clutter ridge, thus suppressing mainlobe and sidelobe clutter.

Figs. 8 and 9 show the two principal cuts of the patterns, corresponding to target Doppler and target azimuth. The azimuth pattern at the target Doppler of 0.25 (cf. Fig. 8) represents the receiver beamformer; and it exhibits nulls at both jammer azimuths (− 20° and 45°) and at the azimuth of 30°, where the sidelobe clutter has the same Doppler as the target. The second cut (Fig. 9) shows the Doppler response at the target azimuth of 20°. The null present at approximately 0.18 Doppler suppresses mainlobe clutter. Finally, the performance of the two STAP processors may be evaluated by plotting the corresponding receiver operating characteristics (ROCs), for two energy detectors that use the adapted weight vectors (see Fig. 10). The ROC curve corresponding to a particular set of adapted weights was calculated via Monte Carlo simulations by using 3 000 independent blocks of data snapshots. The frequency response and ROC comparison in Figs. 7–10 show that the two STAP processors perform comparably for the case of Gaussian interference.

Figs. 11–14 show analogous plots demonstrating the performance of the two methods for a more severe interference environment corresponding to $\alpha = 1.7$. It is demonstrated that the LMP STAP method is more robust against changes in interference. On the other hand, the MVDR STAP method suffers from a raised thermal noise floor

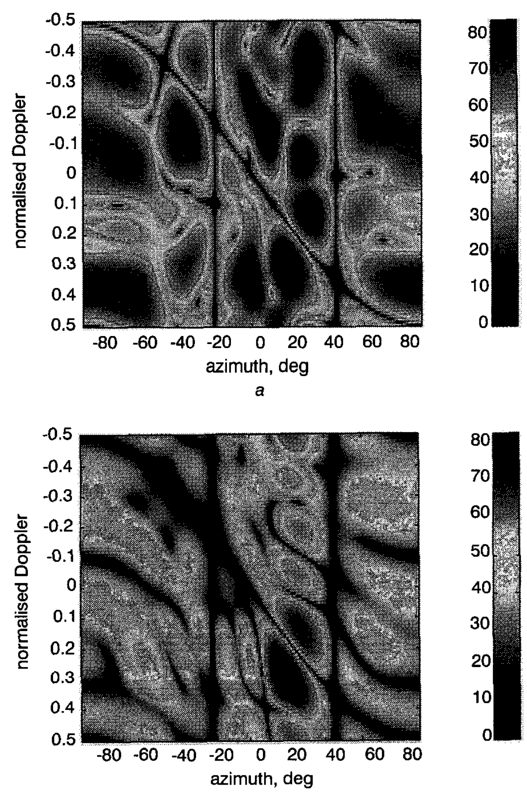

Fig. 11 *Adapted pattern (two-dimensional angle–Doppler frequency responses) for MVDR STAP and LMP STAP*
The presumed target is located at 20° azimuth with normalized Doppler frequency 0.25. The statistics of the clutter (CNR = 30dB) and noise (SNR = 0dB) follow the alpha-stable distribution with $\alpha = 1.70$. Both methods place strong nulls along the two jammers present at − 20° and 45° azimuth and along the clutter ridge, but the LMP STAP exhibits significantly lower sidelobes.
a MVDR STAP
b LMP STAP

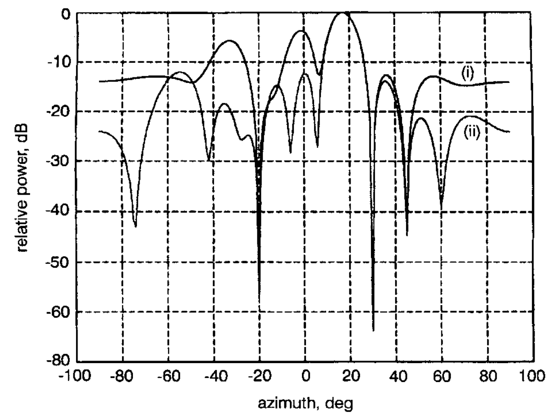

Fig. 12 *Principal cuts at target Doppler*

Note the nulls at both jammer azimuths (– 20° and 45°) and at 30° where the sidelobe clutter has the same Doppler as the target
(i) MVDR STAP; (ii) LMP STAP

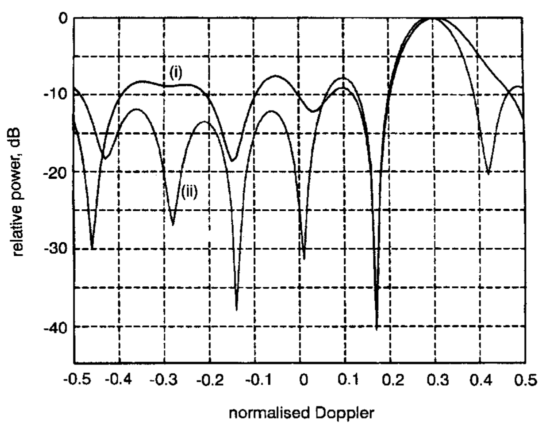

Fig. 13 *Principal cuts at target azimuth*

The null present at approximately 0.18 Doppler suppresses mainlobe clutter
(i) MVDR STAP; (ii) LMP STAP

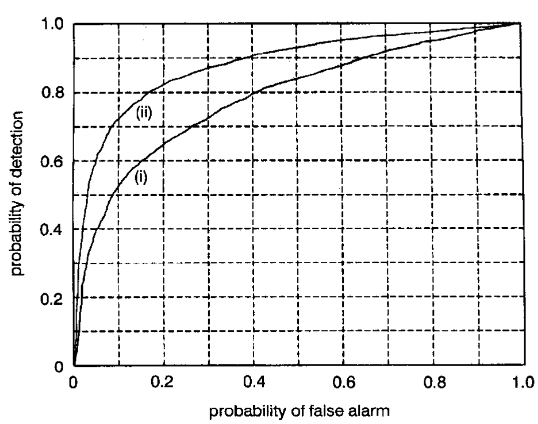

Fig. 14 *Receiver operating characteristics (ROCs) corresponding to the adapted patterns shown in Fig. 11*

(i) MVDR STAP; (ii) LMP STAP

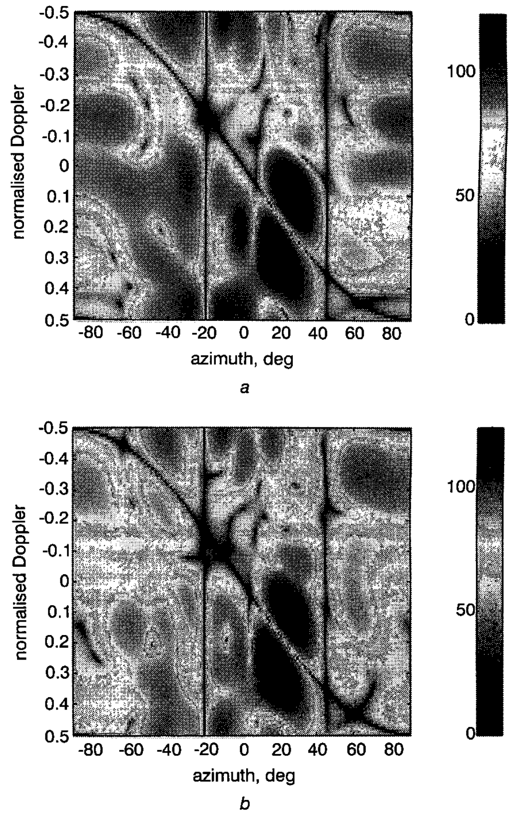

Fig. 15 *Adapted patterns (two-dimensional angle–Doppler frequency responses) for MVDR STAP and LMP STAP*

The presumed target is located at 20° azimuth with normalized Doppler frequency 0.25. The Mountaintop datafile t38pre01v1_cpi_6.mat was used as the additive noise/clutter component (SNR = 0dB). Both methods place strong nulls along the two jammers present at – 20° and 45° azimuth and along the clutter ridge.
a MVDR STAP
b LMP STAP

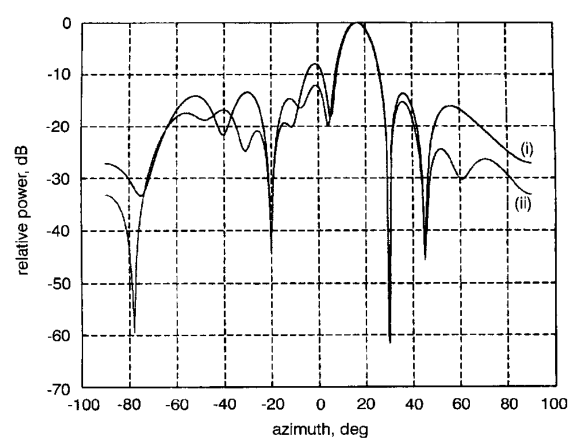

Fig. 16 *Principal cuts at target Doppler*

Note the nulls at both jammer azimuths (– 20° and 45°) and at 30° where the sidelobe clutter has the same Doppler as the target
(i) MVDR STAP; (ii) LMP STAP

with several angle–Doppler regions of high response, with a resulting loss in probability of detection.

Finally, Figs. 15–22 show comparative results by using actual Mountaintop data collected from RSTER, a multiple element array, multiple coherent pulse instrumentation radar system. The datafile t38pre01v1_cpi_6.mat, used as

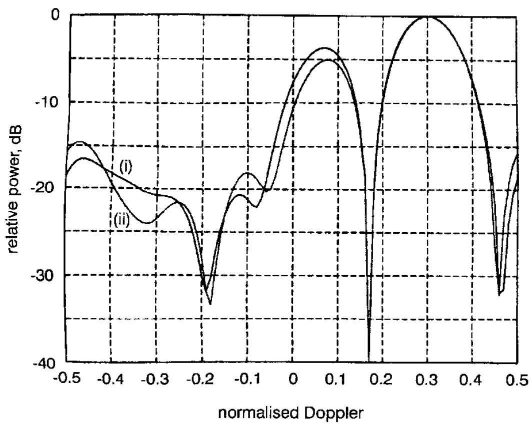

Fig. 17 *Principal cuts at target azimuth*

The null present at approximately 0.18 Doppler suppresses mainlobe clutter
(i) MVDR STAP; (ii) LMP STAP

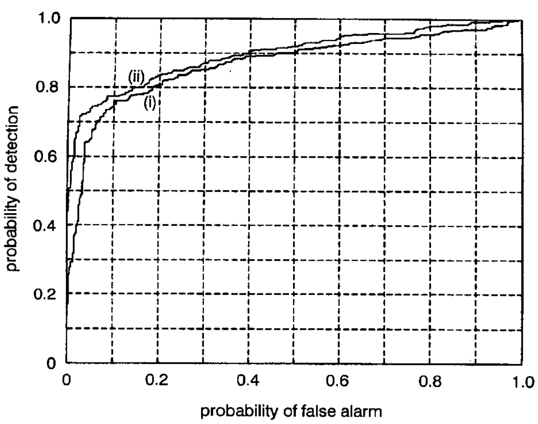

Fig. 18 *Receiver operating characteristics (ROCs) corresponding to the adapted patterns shown in Fig. 15*

(i) MVDR STAP; (ii) LMP STAP

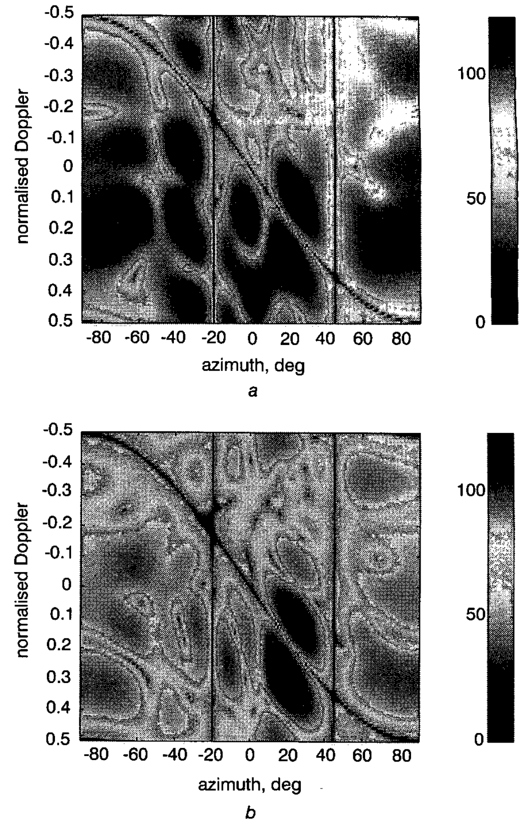

Fig. 19 *Adapted patterns (two-dimensional angle–Doppler frequency responses) for MVDR STAP and LMP STAP*

The presumed target is located at 20° azimuth with normalized Doppler frequency 0.25. The Mountaintop datafile t38pre01v1_cpi_6.mat was used as the additive noise/clutter component (SNR = − 10dB). Both methods place strong nulls along the two jammers present at − 20° and 45° azimuth and along the clutter ridge, but LMP STAP exhibits significantly lower sidelobes.
a MVDR STAP
b LMP STAP

the additive clutter/noise data component, contains ground clutter primarily from a single large scatterer (mountain range) that is isolated in angle. No jammers are present in the datafile, so two artificial barrage jammers were injected into the data at azimuths − 20° and 45°. In addition, a target was added at 20° azimuth with normalised Doppler frequency 0.25. The ROC curves in Figs. 18 and 22 show that an improvement in detection performance is achieved by employing the LMP STAP algorithm.

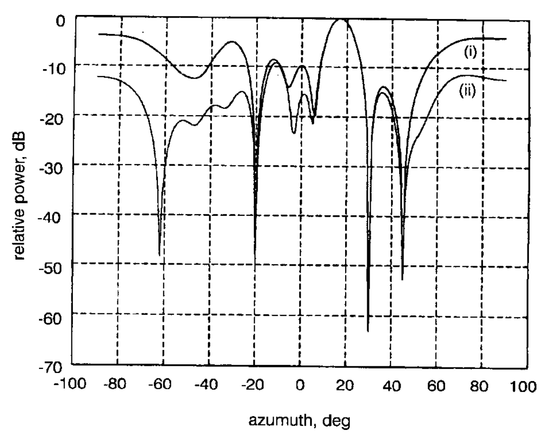

Fig. 20 *Principal cuts at target Doppler*

Note the nulls at both jammer azimuths (− 20° and 45°) and at 30° where the sidelobe clutter has the same Doppler as the target
(i) MVDR STAP; (ii) LMP STAP

6 Conclusions

In this paper, we studied the problem of space-time adaptive processing in severe clutter and interference environments. We showed that the Mountaintop clutter characteristics are non-Gaussian, and can be described accurately with alpha-stable statistical models.

We then, proposed a joint Doppler/channel processing approach for impulsive clutter suppression based on fractional lower-order statistics. We introduced a new constrained adaptive beamformer based on the minimisation of the p-norm of the processor output, in order to adjust an array response to a desired signal while descrimination against impulsive clutter and interference. The results of computer experiments with simulated and actual Mountaintop data series showed that the new technique performs better in localising a target both in space and Doppler, and thus offers the potential for improved airborne radar detection performance.

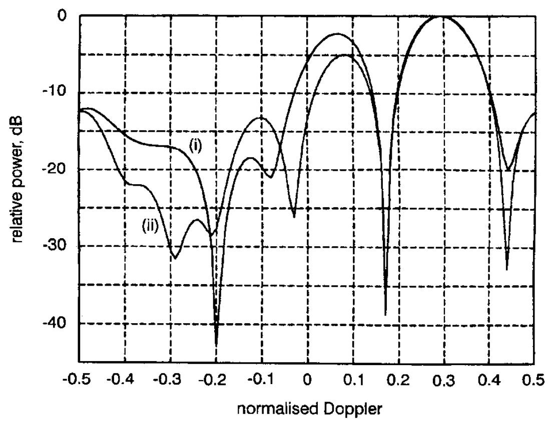

Fig. 21 *Principal cuts at target azimuth*

The null present at approximately 0.18 Doppler suppresses mainlobe clutter
(i) MVDR STAP; (ii) LMP STAP

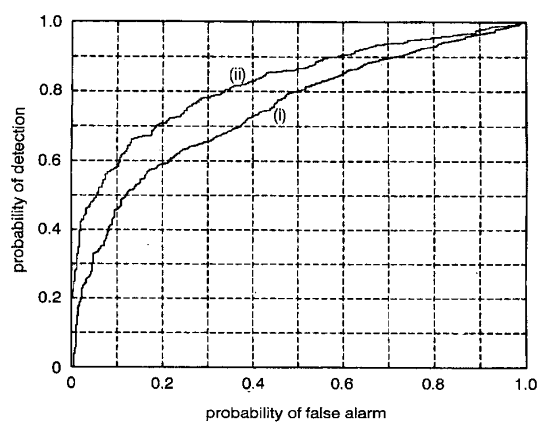

Fig. 22 *Receiver operating characteristics (ROCs) corresponding to the adapted patterns shown in Fig. 19*

(i) MVDR STAP; (ii) LMP STAP

7 Acknowledgments

The work in this paper was supported by Rome Laboratory under Contract F30602-95-1-0001 and by the Office of Naval Research under Contract N00014-98-1-0710.

8 References

1 BRENNAN, L.E., and REED, I.S.: 'Theory of adaptive radar', *IEEE Trans. Aerosp. Electron. Syst.*, 1973, **9**, pp. 237–252
2 REED, I.S., MALLET, J.D., and BRENNAN, L.E.: 'Rapid convergence rate in adaptive arrays', *IEEE Trans. Aerosp. Electron. Syst.*, 1974, **10**, pp. 853–863
3 KELLY, E.J.: 'An adaptive detection algorithm', *IEEE Trans. Aerosp. Electron. Syst.*, 1986, **22**, pp. 115–127
4 BRENNAN, L.E., MALLET, J.D., and REED, I.S., 'Adaptive arrays in airborne MTI', *IEEE Trans. Antennas Propag.*, 1976, **24**, pp. 607–615
5 WARD, J.: 'Cramér-Rao bounds for target angle and Doppler estimation with space-time adaptive processing radar'. Proceedings of 29th Asilomar conference on signals, systems and computers, Pacific Grove, CA, 1995
6 WANG, Y.L., PENG, Y.N., and BAO, Z.: 'Space-time adaptive processing for airborne radar with various array orientations', *IEE Proc., Radar, Sonar Navig.*, 1997, **144**, 330–340
7 PILLAI, S.U., LEE, W.C., and GUERCI, J.: 'Multichannel space-time adaptive processing'. Proceedings of 29th Asilomar conference on signals, systems and computers, Pacific Grove, CA, 1995
8 BARANOSKI, E.J.: 'Improved pre-Doppler STAP algorithm for adaptive clutter nulling in airborne radars'. Proceedings of 29th Asilomar conference on signals, systems and computers, Pacific Grove, CA, 1995
9 KREITHEN, D.E., and STEINHARDT, A.O.: 'Target detection in post-STAP undernulled clutter' Proceedings of Twenty-ninth Asilomar conference on signals, systems and computers,' Pacific Grove, CA, 1995
10 APPLEBAUM, S.P., and CHAPMAN, D.J.: 'Adaptive arrays with main beam constraints,' *IEEE Trans. Antennas Propag.*, 1976, **24**, pp. 650–662
11 WIDROW, B., MANTEY, P.E., GRIFFITHS, L.J.: and GOODE, B.B.: 'Adaptive antenna systems,' *Proc. IEEE*, 1967, **55**, pp. 2143–2159
12 SEKINE, M., OHTANI, S., MUSHA, T., IRABU, T., KIUCHI, E., and HAGISAWA, T.: 'Weibull distributed ground clutter', *IEEE Trans. Aerosp. Electron. Syst.*, 1981, **17**, pp. 596–598
13 RANGASWAMY, M., WEINER, D., and OZTRUK, A.: 'Non-Gaussian random vector identification using spherically invariant random processes', *IEEE Trans. Aerosp. Electron. Syst.*, 1993, **29**, pp. 111–123
14 RAGHAVAN, R.S.: A method for estimating parameters of K-distributed clutter', *IEEE Trans. Aerosp. Electron. Syst.*, 1991, **27**, pp. 238–246
15 FARINA, A., GINI, F., GRECO, M.V., and VERRAZZANI, L.: 'High resolution sea clutter data: statistical analysis of recorded live data', *IEE Proc., Radar, Sonar Navig.*, 1997, **144**, pp. 121–130
16 BALLARD, A.H.: 'Detection of radar signals in log-normal sea-clutter'. Technical Report 7425-8509-T0-000, TRW Sys. Doc., 1996
17 SANGRTON, K.J., and GERLACH, K.R.: 'Coherent detection of radar targets in a non-Gaussian background', *IEEE Trans. Aerosp. Electron. Syst.* 1994, **30**, pp. 330–340
18 CONTE, E., LONGO, M., LOPS, M., and ULLO, S.L.: 'Radar detection of signals with unknown parameters in K-distributed clutter', *IEE Proc. F, Radar Signal Process.*, 1991, **138**, pp. 131–138
19 CONTE, E., LOPS, M., and TULINO, A.M.: 'Hybrid procedure for CFAR in non-Gaussian clutter', *IEE Proc., Radar, Sonar Navig.*, 1997, **144**, pp. 361–369
20 NIKIAS, C.L., and SHAO, M.: 'Signal processing with alpha-stable distributions and applications' (John Wiley, and Sons, New York, 1995)
21 SAMORODNITSKY, G., and TAQQU, M.S., 'Stable non-Gaussian random processes: stochastic, models with infinite variance' (Chapman and Hall, New York, 1994)
22 JANICKI, A., and WERON, A.: 'Can one see α-stable variables and processes', *Stat. Sci.*, 1994, **9**, pp. 109–126
23 TSAKALIDES, P.: 'Array signal processing with alpha stable distributions.' PhD thesis, University of Southern California, Los Angeles, California, 1995
24 TSAKALIDES, P., RASPANTI, R., and NIKIAS, C.L.: 'Joint target angle and doppler estimation in interference modeled as a stable process'. Proceedings of 30th conference on information sciences and systems, Princeton, NJ, 1996
25 TSAKALIDES, P., and NIKIAS, C.L.: 'Joint target angle and doppler estimation with fractional lower-order statistics for airborne radar'. Proceedings of 8th IEEE signal processing workshop on Statistical signal and array processing, Corfu, Greece, 1996
26 SCHILDER, M.: 'Some structure theorems for the symmetric stable laws', *Ann. Math. Stat.*, 1970, **41**, pp. 412–421
27 TSAKALIDES, P., RASPANTI, R., and NIKIAS, C.L.: 'Angle/Doppler estimation in heavy-tailed clutter backgrounds', *IEEE Trans. Aerosp. Electron. Syst.*, April 1999, **35**
28 TITI, G., and MARSHALL, D.: 'The ARPA/NAVY Mountaintop program - Adaptive signal processing for airborne early warning radar'. Proceedings of ICASSP 1996, 1996, Atlanta, GA, pp. 1165–1169
29 WARD, J.: 'Space-time adaptive processing for airborne radar'. Technical Report 1015, Lincoln Laboratory, Dec. 1994
30 FROST, O.L.: 'An algorithm for linearly constrained adaptive array processing', *Proc. IEEE*, 1972, **60**, pp. 926–935
31 CLINE, D.B., and BROCKWELL, P.J.: 'Linear prediction of ARMA processes with infinite variance', *Stoch. Process. Appl.*, 1985, **19**, pp. 281–296
32 TSAKALIDES, P., and NIKIAS, C.L.: 'Robust adaptive beamforming in alpha-stable noise environments'. Proceedings of ICASSP 1996, Atlanta, GA, 1996, pp. 2884–2888
33 TAYLOR, H.L., BANGS, S.C., and McCOY, J.F.: 'Deconvolution with the l_1 norm', *Geophysics*, 1979, **44**, pp. 39–52
34 YARLAGADDA, R., BEDNAR, J.B., and WATT, T.L.: 'Fast algorithms for l_p deconvolution', *IEEE Trans. Acoust. Speech Signal Process.*, 1985, **33**, pp. 174–182
35 SCHROEDER, J., and YARLAGDDA, R.: 'Linear predictive spectral estimation via the l_1 norm', *Signal Process.*, 1989, **17**, pp. 19–29